Contribution from the Division of Chemistry and Chemical Engineering, Arthur Amos Noyes Laboratories, California Institute of Technology, Pasadena, California 91125, and Department of Chemistry, University of Hong Kong, Hong Kong

Monooxo Complexes of Ruthenium(V) as Homogeneous Redox Catalysts for the Electrooxidation of Benzyl Alcohol†

Kwok-Yin Wong,‡ Chi-Ming Che,§ and Fred C. Anson*‡

Received August 28, 1986

The electrochemical behavior of three Ru(IV)–monooxo complexes, *trans*-[Ru^{IV}(TMC)O(X)]ClO_4 (TMC = 1,4,8,11-tetramethyl-1,4,8,11-tetraazacyclotetradecane; X^- = Cl^-, NCO^-, N_3^-), in acetonitrile is described. The formal potentials of the Ru(V)/Ru(IV) couples decrease in the order $Cl^- > NCO^- > N_3^-$. The electrochemically generated Ru(V)–monooxo complexes are active catalysts for the oxidation of benzyl alcohol to benzaldehyde. The rate of benzyl alcohol oxidation decreases in the same order as the formal potentials. The second-order rate constants for reaction between the Ru(V) complexes and benzyl alcohol were evaluated by rotating disk voltammetry. The values obtained were 2.1×10^2 and 1.4×10^2 M^{-1} s^{-1} for X^- = Cl^- and NCO^-, respectively. The catalysts gradually lose their activity during the course of the electrooxidation of benzyl alcohol because of what appears to be decomposition of the catalysts during the period that they are in the Ru(V) oxidation state.

The study of ruthenium–oxo complexes as active electrocatalysts is a matter of current interest.[1-3] The electrooxidation of benzyl alcohol in acetonitrile as catalyzed by *trans*-[Ru^{V}(TMC)O(Cl)]$^{2+}$ (TMC = 1,4,8,11-tetramethyl-1,4,8,11-tetraazacyclotetradecane) has previously been communicated.[2] Although the catalyst is not long-lived, we reasoned that changes in the ligand trans to the axial oxygen atom might improve the stability and/or enhance the reactivity of these ruthenium oxo complexes. The syntheses of two new Ru(IV)–monooxo complexes *trans*-[Ru^{IV}(TMC)O(NCO)]ClO_4 and *trans*-[Ru^{IV}(TMC)O(N_3)]ClO_4 were therefore undertaken.[4] The electrochemical behavior of these new Ru(IV)–monooxo complexes in acetonitrile and the catalytic properties of the corresponding Ru(V) complexes toward the oxidation of benzyl alcohol are described in this report.

Experimental Section

Materials. The synthesis of *trans*-[Ru^{IV}(TMC)O(Cl)]ClO_4 followed a previously reported scheme[2] with slight modification: *trans*-[Ru^{VI}(TMC)O_2]$(ClO_4)_2$[3] (0.85 mmol), *n*-$(C_4H_9)_4NCl$ (0.85 mmol), and excess triphenylphosphine (8.4 mmol) were stirred in acetone (30 mL) at room temperature for 1 h. A deep yellow solution was obtained. A 1.5-g sample of *n*-$(C_4H_9)_4NClO_4$ was then added to the solution followed by anhydrous diethyl ether to precipitate *trans*-[Ru^{IV}(TMC)O(Cl)]ClO_4 as a yellow solid. The crude product was collected by filtration and purified by slow diffusion of diethyl ether into an acetone solution of the crude product (yield 80%). UV–vis spectrum in CH_3CN (λ_{max}, nm (ϵ, cm^{-1} dm^3 mol^{-1})): 460 (130), 295 (2300). Anal. Calcd: C, 33.1; H, 6.3; N, 11.0; Cl, 14.0. Found: C, 33.5; H, 6.6; N, 11.4; Cl, 14.0. The synthesis and crystal structures of *trans*-[Ru^{IV}(TMC)O(NCO)]ClO_4 and *trans*-[Ru^{IV}(TMC)O(N_3)]ClO_4 will be reported in a subsequent paper.[4] UV–vis spectrum in CH_3CN (λ_{max} (ϵ, cm^{-1} dm^3 mol^{-1})): *trans*-[Ru^{IV}(TMC)O(NCO)]ClO_4, 460 (120), 295 (4600); *trans*-[Ru^{IV}(TMC)O(N_3)]ClO_4 ~ 375 (sh) (~ 3000), 355 (3300). Acetonitrile (Burdick and Jackson) was distilled over CaH_2 under argon before use. Tetraethylammonium fluoborate (Southwestern Analytical Chemicals) was dried in vacuo for 24 h at 100 °C. Glassy-carbon electrodes were constructed by pressure-fitting 5-mm rods (Tokai) into Teflon supports. The exposed surfaces (0.20 cm^2) were polished with 0.3-μm alumina paste, washed thoroughly with water, sonicated for 5 min in pure water, rinsed with acetonitrile, and dried. Laboratory-distilled water was purified by passing it through a purification train (Barnstead Nanopure). Other chemicals were reagent grade and used as received.

Apparatus and Techniques. Cyclic voltammetry was performed with appropriate PAR instrumentation and an X-Y recorder. Rotating disk current–potential curves were obtained with a Tacussel electrode and rotator (Model EDI), which had an operating range of 100–5000 rpm. Potentials were controlled with respect to a Ag^+/Ag reference electrode in acetonitrile but are reported with respect to the ferrocenium/ferrocene couple ($Cp_2Fe^{+/0}$) as measured in the same solution.[5] Experiments were conducted at the ambient laboratory temperature (22 ± 2 °C). Elemental analyses were performed by the Microanalytical Unit of the Australian Mineral Development Laboratories (Melbourne, Australia).

Table I. Formal Potentials in Acetonitrile for the Ru(V)/Ru(IV) Couples of the Complexes Examined in This Study[a]

complex	E_f,[b] V vs. $Cp_2Fe^{+/0}$
trans-[Ru(TMC)O(Cl)]ClO_4	1.05
trans-[Ru(TMC)O(NCO)]ClO_4	0.89
trans-[Ru(TMC)O(N_3)]ClO_4	0.72

[a] Supporting electrolyte: 0.1 M tetraethylammonium fluoborate. Glassy-carbon electrode. [b] Potentials are referenced to the ferrocenium/ferrocene couple in the same solution.

Results and Discussion

Voltammetry of *trans*-[Ru^{IV}(TMC)O(X)]$^+$ (X^- = Cl^-, NCO^-, N_3^-). Cyclic voltammograms of these three monooxo–Ru(IV) complexes contain a prominent oxidation wave in the range 0.7–1.1 V vs. $Cp_2Fe^{+/0}$ (Figure 1). Corresponding reduction waves are present to establish the reversibility of the couples at the scan rates employed. The formal potentials of the three couples, taken as the average of the cyclic voltammetric peak potentials, are listed in Table I and show a considerable dependence on X^-, decreasing in the order $Cl^- > NCO^- > N_3^-$. The ruthenium ion is the most likely site of the redox process because the metal-bound, saturated tertiary amine ligand shows no anodic activity in the range of potentials involved.[6]

Attempts to generate solutions of the Ru(V)–monooxo complexes by controlled-potential oxidation of the Ru(IV) precursors were unsuccessful with all three complexes. New species with λ_{max} values in the range 420–370 nm were generated during the electrolyses, but the spectra were not stable and isosbestic points were not observed.

At a scan rate lower than that employed to record the voltammograms in Figure 1 the *trans*-[Ru^{IV}(TMC)O(Cl)]$^+$ complex, but not the corresponding cyanato and azido complexes, exhibits a split cathodic wave (Figure 2). X-ray crystallographic data show that the chloride ligand is weakly bound to the ruthenium center[2] so that the double cathodic wave may be the result of a

* To whom correspondence should be addressed.
† Contribution No. 7465. from the Arthur Amos Noyes Laboratories.
‡ California Institute of Technology.
§ University of Hong Kong.

(1) See, for example: (a) Moyer, B. A.; Thompson, M. S.; Meyer, T. J. *J. Am. Chem. Soc.* **1980**, *102*, 2310. (b) Samuels, G. J.; Meyer, T. J. *J. Am. Chem. Soc.* **1981**, *103*, 307. (c) McHatton, R. C.; Anson, F. C. *Inorg. Chem.* **1984**, *23*, 3935. (d) Kutner, W.; Meyer, T. J.; Murray, R. W. *J. Electroanal. Chem. Interfacial Electrochem.* **1985**, *195*, 375.
(2) Che, C. M.; Wong, K. Y.; Mak, T. C. W. *J. Chem. Soc., Chem. Commun.* **1985**, 988.
(3) Che, C. M.; Wong, K. Y.; Poon, C. K. *Inorg. Chem.* **1985**, *24*, 1797.
(4) Che, C. M.; Lai, T. F.; Wong, K. Y., to be submitted for publication.
(5) Gritzner, G.; Kuta, J. *Pure Appl. Chem.* **1982**, *54*, 1527. Gagne, R. R.; Koval, C. A.; Lisensky, G. C. *Inorg. Chem.* **1980**, *19*, 2854.
(6) Wong, K. Y. Ph.D. Thesis, University of Hong Kong, 1986.

0020-1669/87/1326-0737$01.50/0

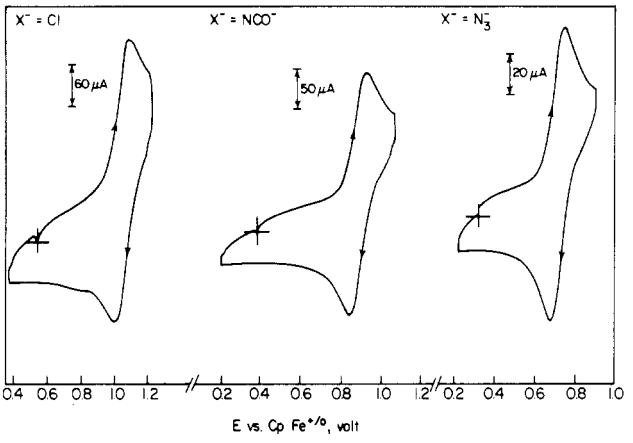

Figure 1. Cyclic voltammograms for 1 mM *trans*-$[Ru^{IV}(TMC)O(X)]^+$ in acetonitrile at glassy-carbon electrodes: $X = Cl^-$, scan rate = 1 V s^{-1}; $X = NCO^-$, scan rate = 0.5 V s^{-1}; $X^- = N_3^-$, scan rate = 0.1 V s^{-1}. Supporting electrolyte: 0.1 M tetraethylammonium fluoborate.

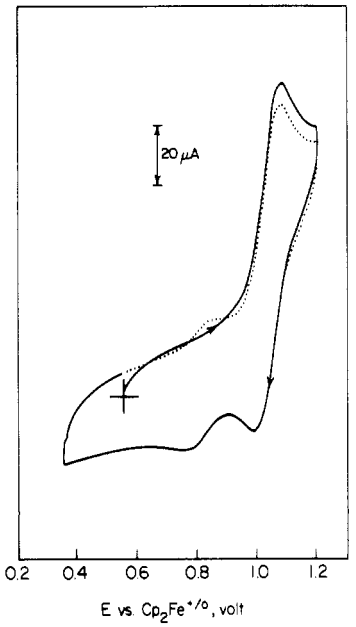

Figure 2. Cyclic voltammogram for 1 mM *trans*-$[Ru^{IV}(TMC)O(Cl)]^+$ recorded at 0.1 V s^{-1}: First scan, solid line; second scan, dotted line. Other conditions are as in Figure 1.

relatively rapid release of chloride by the oxidized complex to produce a mixture of complexes at the surface of the electrode. Evidence for a similar but slower reaction with the cyanato (but not the azido) complex was obtained by repetitive scanning at 0.1 V s^{-1}. After about 10 scans, a small reversible response appeared that was centered at 0.74 V. The new reversible responses obtained with the chloro and cyanato complexes have different formal potentials that cannot be attributed to a single, common intermediate such as the oxo acetonitrile complex. This complex can also be ruled out because it exhibits no electroactivity in the potential range of interest. Even when both forms of the Ru(IV) complex are present in solution, the oxidation of benzyl alcohol does not commence until the electrode potential is scanned to the second, more positive, oxidation wave where the original chloro complex is oxidized. Thus, the species responsible for the new waves are not catalysts for the oxidation of benzyl alcohol. However, their identities are of interest as examples of relatively rare complexes of Ru(V), and attempts to characterize them are under way.

Current–potential curves for the three complexes recorded at the rotating disk electrode yield anodic plateau currents comparable to that obtained for ferrocene at the same concentration, indicating that a one-electron oxidation of Ru(IV) to Ru(V) is involved. Levich plots[7] of the plateau current vs. the square root of the rotation rate are straight lines that pass through the origin and have slopes from which reasonable values for diffusion coefficients were calculated (1.55, 1.31, and 1.29 × 10^{-5} cm^2 sec^{-1} for $X^- = Cl^-$, NCO^-, and N_3^-, respectively), assuming a one-electron oxidation.

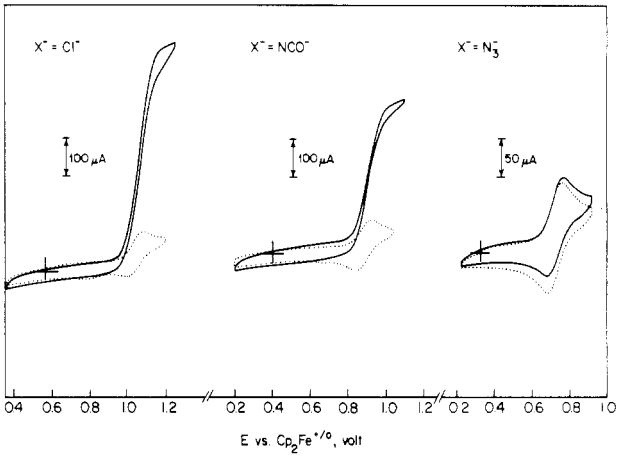

Figure 3. Cyclic voltammograms for the oxidation of 1 mM *trans*-$[Ru(TMC)O(X)]^+$ in the presence of 0.1 M benzyl alcohol. Scan rate = 0.1 V s^{-1}. Other conditions are as in Figure 1. The dashed curves show the voltammograms in the absence of alcohol.

Catalytic Oxidation of Benzyl Alcohol. Benzyl alcohol is not oxidizable at glassy-carbon electrodes at potentials less positive than 1.2 V. However, significant anodic currents flow upon addition of *trans*-$[Ru^{IV}(TMC)O(X)]^+$ ($X^- = Cl^-$ or NCO^-), and the catalytic current rises at the potential where the complexes are oxidized to Ru(V) (Figure 3). The azido complex, with the least oxidizing formal potential, is also the poorest catalyst, yielding currents in the presence of benzyl alcohol only slightly larger than those for the catalyst alone (Figure 3).

The anodic portions of the voltammograms for $X^- = Cl^-$ or NCO^- in Figure 3 are approaching the flat-topped shape that is expected in the presence of a large excess of substrate with electrogenerated catalysts that react slowly enough to consume very little of the substrate but rapidly enough to establish a stationary concentration of catalyst at the electrode surface.[8] Under such conditions, limiting currents that are independent of scan rate are expected that can be used to calculate the rate constant for the homogeneous cross-reaction between substrate and catalyst if a simple pseudo-first-order reaction is assumed[8]

$$i = FD_P^{1/2}C_P(2kC_A)^{1/2} \quad (1)$$

where i is the limiting current density, F is Faraday's constant, D_P and C_P are the diffusion coefficient and concentration, respectively, of the catalyst, C_A is the substrate concentration, k is the second-order rate constant, and the factor of $(2)^{1/2}$ accounts for the two-electron character of the catalyzed reaction. The experimental limiting currents were almost independent of scan rate at a rate of 0.1 V s^{-1} from which approximate rate constants of 2.6 × 10^2 and 1.3 × 10^2 M^{-1} s^{-1} were calculated from eq 1 for the chloro and cyanato complexes, respectively.

Bulk electrolyses of solutions containing 0.39 M benzyl alcohol and 3 mM catalyst were carried out with large-area platinum or glassy-carbon electrodes held at a potential 100 mV positive of the formal potential of the catalyst (chloro or cyanato). Analysis of the oxidation products by gas chromatography and mass spectrometry showed that the oxidation produced benzaldehyde with over 90% current efficiency. The complexes were shown to be impotent as catalysts for the oxidation of benzaldehyde, which is consistent with the high current efficiency observed.

(7) Levich, V. G. *Physicochemical Hydrodynamics*; Prentice Hall: Englewood Cliffs, NJ, 1962; Chapter 1, p 69.
(8) Andrieux, C. P.; Blocmar, C.; Dumas-Bouchiat, J. M.; M'Halla, F.; Saveant, J.-M. *J. Electroanal. Chem. Interfacial Electrochem.* **1980**, *113*, 19.

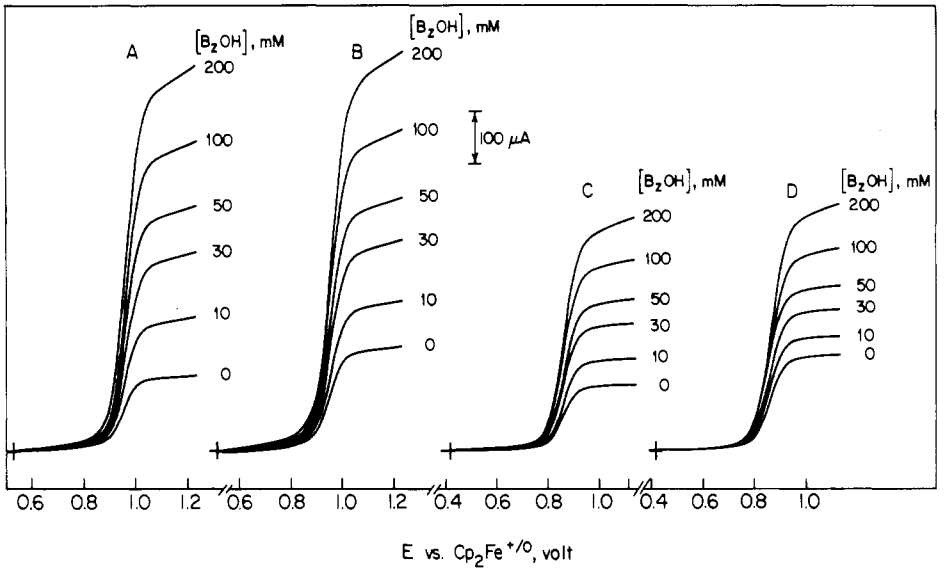

Figure 4. Current–potential curves for the oxidation of benzyl alcohol (BzOH) in acetonitrile at a rotating glassy-carbon disk electrode as catalyzed by (A, B) 1 mM trans-$[Ru^{IV}(TMC)O(Cl)]^+$ and (C, D) *trans*-$[Ru^{IV}(TMC)O(NCO)]^+$. Rotation rate: (A, C) 450 rpm; (B, D) 933 rpm. Electrode potential was scanned at 5 mV s^{-1}. Supporting electrolyte: 0.1 M tetraethylammonium fluoborate.

Table II. Kinetic Data for the Electrooxidation of Benzyl Alcohol (BzOH) As Catalyzed by *trans*-$[Ru^V(TMC)O(Cl)]^{2+}$ and *trans*-$[Ru^V(TMC)O(NCO)]^{2+}$ [a]

[BzOH], mM	γ [b]	ω [c] = 450 rpm CAT [d]	log k [e]	ω = 933 rpm CAT	log k	ω = 1415 rpm CAT	log k	ω = 1901 rpm CAT	log k	ω = 2384 rpm CAT	log k
					trans-$[Ru^V(TMC)O(Cl)]^{2+}$						
20	2	0.20	2.30 (2.37)	0.13	2.38 (2.40)	0.085	2.37 (2.37)	0.075	2.40 (2.38)	0.060	2.40 (2.38)
50	5	0.15	2.22 (2.30)	0.11	2.35 (2.41)	0.075	2.36 (2.32)	0.065	2.41 (2.35)	0.049	2.38 (2.31)
100	10	0.12	2.20 (2.25)	0.075	2.24 (2.27)	0.060	2.30 (2.28)	0.047	2.30 (2.28)	0.039	2.31 (2.28)
200	20	0.07	2.00 (2.01)	0.048	2.10 (2.10)	0.036	2.10 (2.20)	0.030	2.13 (2.17)	0.025	2.15 (2.22)
					trans-$[Ru^V(TMC)O(NCO)]^{2+}$						
20	2	0.18	2.21 (2.30)	0.11	2.27 (2.30)	0.080	2.32 (2.32)	0.060	2.32 (2.32)	0.050	2.33 (2.30)
50	5	0.14	2.14 (2.20)	0.085	2.21 (2.20)	0.065	2.26 (2.24)	0.050	2.26 (2.25)	0.044	2.20 (2.19)
100	10	0.090	2.00 (2.03)	0.060	2.10 (2.11)	0.046	2.13 (2.05)	0.037	2.15 (2.04)	0.032	2.18 (2.04)
200	20	0.055	1.82 (1.84)	0.037	1.90 (1.90)	0.029	1.95 (2.00)	0.024	1.97 (1.95)	0.021	2.00 (2.04)

[a] Supporting electrolyte: 0.1 M tetraethylammonium fluoborate in acetonitrile. Glassy-carbon electrode. [b] Ratio of the concentrations of BzOH to catalyst. [c] Rate of rotation of the rotating disk electrode. [d] $CAT = (i_{exptl} - i_L)/2\gamma i_L$. [e] Rate constants were calculated from the equation on p 5 of ref 9 (see text). The values in parentheses were evaluated from Figure 1 of ref 9.

Catalyzed oxidations of benzyl alcohol at the rotating disk electrode are shown in Figure 4. The plateau currents exceed the Levich current,[7] increase with the concentration of alcohol and decrease as the rotation rate is increased. Summarized in Table II are data obtained with the chloro and cyanato catalysts at a series of benzyl alcohol concentrations. (The catalytic activity of the azido complex was too small to measure reliably even in 0.5 M benzyl alcohol solutions.) The catalytic efficiency, CAT, is defined by Andrieux et al.[9] for reactions involving a single electron

$$CAT \equiv (i_{exptl} - i_L)/\gamma i_L \qquad (2)$$

where i_{exptl} is the experimental plateau current, i_L is the convection–diffusion-limited Levich current for the catalyst alone at the same rotation rate, and γ, the excess factor, is the ratio of the substrate to the catalyst concentrations. For substrates that undergo two-electron reactions the appropriate definition of CAT requires that the right-hand side of eq 2 be multiplied by 0.5. The data in Table II show that the values of CAT decrease with the electrode rotation rate and the excess factor. This behavior is typical of a catalytic reaction coupled to the electrode reaction. To utilize the data to evaluate the kinetics of the reaction it is necessary to propose a likely reaction mechanism and to compare the concentration and rotation rate dependences calculated on the basis of the mechanism with those observed experimentally.[9] A possible mechanism for the present case is given in reactions 3–5

Table III. Concentration Dependence of Catalytic Efficiencies at Constant Excess Factor (γ = 10) and Rotation Rate (ω = 450 rpm)

[BzOH], mM	catalytic efficiency: *trans*-$[Ru^{IV}(TMC)O(Cl)]^+$	*trans*-$[Ru^{IV}(TMC)O(NCO)]^+$
10	0.033	0.017
30	0.060	0.040
50		0.055
100	0.125	0.090

$$Ru^{IV} - e^- \rightleftarrows Ru^V \qquad (3)$$

$$Ru^V + PhCH_2OH \xrightarrow{k} Ru^{IV} + PhCHOH + H^+ \qquad (4)$$

$$Ru^V + PhCHOH \xrightarrow{fast} Ru^{IV} + PhCHO + H^+ \qquad (5)$$

where the catalyst is abbreviated as Ru^{IV} or Ru^V. The close correspondence between the potentials where Ru(IV) is oxidized to Ru(V) in the absence of benzyl alcohol and the potential where the catalytic oxidation occurs implicates Ru(V) as the catalytically active oxidation state. Thus, half-reaction 3 followed by reaction 4 are the likely initial steps in the catalytic cycle. Possible alternatives to reaction 5 include oxidation of the benzyl alcohol radical at the electrode surface or oxidation by Ru(IV) instead of Ru(V). The oxidation of PhCHOH at the electrode surface

(9) Andrieux, C. P.; Dumas-Bouchiat, J. M.; Saveant, J.-M. *J. Electroanal. Chem. Interfacial Electrochem.* **1980**, *113*, 1.

Table IV. Formal Potentials or Cathodic Peak Potentials of *trans*-$[Ru(TMC)XY]^{n+}$ in CH_3CN

		potential, V vs. $Cp_2Fe^{+/0}$						
X	Y	Ru(III)/Ru(II)	Ru(IV)/Ru(III)	Ru(V)/Ru(IV)	Ru(VI)/Ru(V)	oxidn state	reactivity toward BzOH[d]	ref
Cl	Cl	−0.62[a]	1.15			IV	0	11
Br	Br	−0.42[a]	1.17					11
NCO	NCO	−0.59	1.07					11
CH_3CN	CH_3CN	0.76						11
O	Cl	[c]	−1.34[a,b]	1.05		V	++	6, this work
O	NCO		−1.26[b]	0.89		V	++	6, this work
O	N_3		−1.29[b]	0.72		V	+	6, this work
O	CH_3CN		−0.86[a,b]			IV	0	6
O	O	−1.89	−1.61[a]	−1.24	−0.12	VI	0	6

[a] Irreversible; the recorded potential is the cathodic peak potential at a scan rate of 100 mV s^{-1}. [b] The waves obtained probably involve several electrons. [c] The absence of an entry indicates that no voltammetric wave was observed within the accessible potential range. [d] Qualitative comparison of the reaction rates of the complex in the indicated oxidation state with benzyl alcohol (~100 mM) in acetonitrile at room temperature. Reactivity code: (++) reacts readily; (+) modest reaction rate; (0) very slow or no reaction. The absence of an entry denotes that the reaction rate has not been tested.

is not likely because the rate constant for reaction 4 is relatively low (vide infra) so that Ru(V) generated at the electrode will diffuse away from surface before significant reaction with benzyl alcohol occurs. As a result, most of the PhĊHOH radicals are formed too far from the electrode surface to be oxidized directly.[10]

For the oxidation of benzyl alcohol radical by Ru(IV) to proceed rapidly the potential of the PhCHO/PhĊHOH couple would have to be considerably more negative than −1.2 V vs. $Cp_2Fe^{+/0}$ where the reduction of Ru(IV) occurs.[11] A formal potential for the PhCHO/PhĊHOH couple is not available but since the formal potential of the Ru(V)/Ru(IV) couple is over 2 V more positive than that for the Ru(IV)/Ru(III) couple, Ru(V) seems more likely than Ru(IV) as the oxidant of the PhĊHOH radicals. We therefore analyzed the kinetic data on the basis of the mechanism embodied in reactions 3–5. The mechanism is of the type labeled SET (solution electron transfer) by Andrieux et al.[9] and treated theoretically by them. The kinetic process controlling the current was identified as reaction 4 by measuring the catalytic efficiency, CAT, as a function of catalyst concentration at a constant ratio of substrate (benzyl alcohol) to catalyst.[9] The values of CAT increased with the substrate concentration (Table III), which shows that the system falls in the KE or KG regions of the relevant kinetic zone diagram (Figure 6 of ref 9). If, as seems likely, the rate of reaction 5 is much greater than that of the reverse of reaction 4, the system falls in the KE region for which working curves relating catalytic efficiencies to the (forward) rate constant for reaction 4 have been calculated by Andrieux et al.[9] The data in Table II were analyzed by means of the working curves in Figure 1 of ref 9, and by direct calculation using the unnumbered equation in the middle of p 5 of ref 9, which was applicable under most of the experimental conditions employed.[9] The working curves corresponding to twice the experimental excess factors were employed, and the CAT values were calculated as $(i_{expt} - i_L)/2\gamma i_L$ to take account of the two-electron character of the reaction.[9] Similarly, γ was replaced by 2γ in the equation from ref 9 when it was used to evaluate rate constants. Rate constants for reaction 4 obtained by both procedures are listed in Table II. At each value of the excess factor, γ, the rate constants are reasonably independent of the electrode rotation rate, indicating that the rate of reaction 4 is first order in catalyst as was assumed in the derivation in ref 9. There is a slight trend toward smaller values at lower rotation rates in the rate constants evaluated from the equation from ref 9 instead of the working curves in Figure 1 of the same reference. This equation is expected to provide a less and less accurate description of the kinetic situation as the rotation rate decreases,[9] and the trend observed is probably a reflection of this fact. The rate constants obtained under the same reaction conditions as were used to record Figure 4, $k = 2.1 \times 10^2$ and 1.4×10^2 M^{-1} s^{-1} for the chloro and cyanato complexes, respectively, are in reasonable agreement with the approximate rate constants obtained earlier from eq 1 and the limiting currents in Figure 3. This adds support to the conclusion that the reaction rate law is first order in catalyst.

The rate constants in Table II remain independent of the excess factor for small values of γ but appear to decrease somewhat at benzyl alcohol concentrations of 100 mM or higher. This trend may arise from changes in the bulk properties of the reaction medium, e.g., viscosity, at higher benzyl alcohol concentrations.

Catalyst Deactivation. The catalysts gradually lose their activity during the course of electrooxidations of benzyl alcohol. For example, after 18 catalyst turn-overs (ca. 60 min) with a 0.39 M solution of benzyl alcohol and 1 mM catalyst, the initial oxidation current decreased 2-fold with *trans*-$[Ru^{IV}(TMC)O(NCO)]^+$ and 10-fold with *trans*-$[Ru^{IV}(TMC)O(Cl)]^+$. We attribute the loss in activity to the spoiling decomposition reactions that the catalysts undergo when oxidized to the Ru(V) states as revealed, for example, in the cyclic voltammogram of the chloro catalyst in Figure 2.

Relative Rates and Comparison with Other Ru(V) Complexes. The rate constants measured for the chloro catalyst are about 50% larger than those for the cyanato catalyst, which is not surprising since the latter complex is also a somewhat weaker oxidant (Table I). However, extrapolation of this trend to the azido complex would lead to an expected rate constant only 2-fold smaller than that of the chloro catalyst. In fact, the rate constant was too small to measure, which, for our experimental conditions, meant $k < 1$ M^{-1} s^{-1}. Thus, the oxidizing strength of these complexes is apparently not the primary factor involved in determining their relative catalytic activities.

Comparisons with the behavior of related ruthenium–TMC complexes adds support to this conclusion: *trans*-$[Ru^{IV}(TMC)Cl_2]^{2+}$ with a formal potential for the Ru(IV)/Ru(III) couple of 1.15 V vs. $Cp_2Fe^{+/0}$[11] is a stronger oxidant than *trans*-$[Ru^{V}(TMC)OCl]^{2+}$ but a poorer catalyst for the electrooxidation of both isopropyl[11] and benzyl[12] alcohols. (The oxidation of *trans*-$[Ru^{IV}(TMC)Cl_2]^{2+}$ to the Ru(V) state was not observable within the accessible potential range so that *trans*-$[Ru^{V}(TMC)Cl_2]^{3+}$ is presumably a very powerful oxidant whose reactivity toward alcohol oxidations is untested.)

The presence of the oxo ligand appears to be necessary but insufficient to obtain an active catalyst. For example, *trans*-$[Ru^{VI}(TMC)(O)_2]^{2+}$[3] and *trans*-$[Ru^{V}(TMC)(O)_2]^{+}$[13] are both relatively unreactive toward benzyl alcohol despite the high oxidation state of the ruthenium.[14] The reason is doubtless the relatively weak oxidizing power of the complexes. The formal potentials for the Ru(VI)/Ru(V) and Ru(V)/Ru(IV) couples in

(10) Saveant, J.-M.; Su, K. B. *J. Electroanal. Chem. Interfacial Electrochem.* **1985**, *196*, 1.
(11) Che, C. M.; Wong, K. Y.; Poon, C. K. *Inorg. Chem.* **1986**, *25*, 1809.
(12) Che, C.-M.; Wong, K. Y., unpublished experiments.
(13) Che, C. M.; Wong, K. Y. *J. Chem. Soc., Chem. Commun.* **1986**, 229.
(14) The second-order rate constant for the reaction between *trans*-$[Ru^{VI}(TMC)(O)_2]^{2+}$ and benzyl alcohol in acetonitrile is 2×10^{-4} mol^{-1} dm^3 s^{-1} at 25 °C. The corresponding Ru(V) complex appeared unreactive toward benzyl alcohol.

acetonitrile are −0.12 and −1.24 V vs. $Cp_2Fe^{+/0}$, respectively.

Table IV summarizes the formal potentials and reactivity toward the oxidation of alcohols of a series of ruthenium–TMC complexes in various oxidation states. One generalization that emerges from these data is that the monooxo complexes of Ru(V) are the most active catalysts with the ligand trans to the oxo ligand exerting a very strong effect on the reactivity.

The fact that the rates of the catalyzed oxidations of alcohols do not respond simply to changes in the oxidizing strength of the catalyst argues against an outer-sphere mechanism for the catalyzed reaction. Since reaction 4 involves the transfer of both a proton and an electron (or a hydrogen atom) from the alcohol, it is tempting to regard the oxo ligand as facilitating the transfers by helping to stabilize the departing proton. The ability of the oxo ligand to function in this way could well be strongly influenced by the nature of the other trans ligand, with saturated ligands such as chloride being preferable to ligands such as oxo or azido because of potential $p\pi$(ligand)–$d\pi^*$(Ru)–$p\pi$(O) interactions. This would provide a rationalization for reactivities that do not correlate simply with the formal potentials of the catalysts.

The chemistry of mononuclear Ru(V)–oxo complexes is relatively unexplored,[15] and studies with a greater variety of trans ligands will be necessary to provide less speculative interpretations of the catalytic reactivity patterns that have been encountered.

Acknowledgment. This work was supported by the U.S. National Science Foundation (Caltech) and the Committee on Conference and Research grants of the University of Hong Kong.

(15) See, for example: Seddon, E. A.; Seddon, K. R. In *The Chemistry of Ruthenium*; R. J. H., Clark, Ed.; Elsevier: Amsterdam, 1984; Chapter 6.

Contribution from the Departments of Chemistry, McMaster University, Hamilton, Ontario L8S 4M1, Canada, and University of Toronto, Toronto, Ontario M5S 1A1, Canada

Dilead(II) Chalcogenide Anions $Pb_2Ch_3^{2-}$ (Ch = Se, Te): A ^{207}Pb, ^{125}Te, and ^{77}Se Solution NMR Study. X-ray Crystal Structure of (2,2,2-crypt-K^+)$_2Pb_2Se_3^{2-}$

Mår Björgvinsson,[†] Jeffery F. Sawyer,[‡] and Gary J. Schrobilgen*[†]

Received June 16, 1986

A new series of dilead(II) chalcogenide anions, $Pb_2Ch_3^{2-}$ (Ch = Se, Te), has been obtained by extraction of the appropriate ternary or quaternary Zintl phases of the type $KPb_xSe_{(3-n)/3}Te_{n/3}$ (where $x \approx {}^1/_2$ and n = 0–3) with ethylenediamine (en) in the presence of 2,2,2-crypt and have been characterized in en solution by ^{207}Pb, ^{125}Te, and ^{77}Se NMR spectroscopy. The coupling constants $^1J_{^{207}Pb-^{125}Te}$ and $^1J_{^{207}Pb-^{77}Se}$ have been determined for all four possible anions, $Pb_2Se_xTe_{3-x}^{2-}$ (x = 0–3), enabling structural comparisons within the series after the nuclear dependence has been removed to give reduced coupling constants $^1K_{Pb-Te}$ and $^1K_{Pb-Se}$. Allowances have also been made for relativistic effects, which are of major importance in heavy-element spin–spin coupling and in the series of anions under consideration. The NMR findings indicate that the structures of the anions are based upon a trigonal bipyramid having axial lead atoms bonded to three chalcogen atoms in the equatorial plane and are supported by the X-ray crystal structure of (2,2,2-crypt-K^+)$_2Pb_2Se_3^{2-}$, which has been determined at room temperature. This compound crystallizes in the monoclinic system, space group $P2_1/n$, with four molecules in a unit cell of dimensions a = 10.320 (4) Å, b = 47.011 (11) Å, c = 11.430 (4) Å, and β = 90.25 (4)°, with R = 0.1184 for 3956 observed ($I > 3\sigma(I)$) reflections. In addition to eight 2,2,2-crypt-K^+ cations, the structure also contains four trigonal-bipyramidal $Pb_2Se_3^{2-}$ anions per unit cell with essentially D_{3h} symmetry. The Pb–Se distances are 2.726 (5)–2.792 (8) Å with Pb–Se–Pb angles of 70.4 (1)–70.9 (1)° and Se–Pb–Se angles of 87.1 (2)–91.6 (1)°. The distance between the two axial lead atoms is only 3.184 (3) Å and is substantially less than the accepted van der Waals contact.

Introduction

Although much of the earlier work on Zintl anions has produced cluster, cage, or ring cluster species, numerous examples of heteroatomic classically bonded anions extracted from Zintl alloys have come to light. (For an excellent recent review of these topics, see ref 1). It is apparent in the recent literature that extraction of Zintl alloys of mixtures of electropositive elements such as Hg, Tl, Sn, with As and electronegative elements such as Se and Te in ethylenediamine produces classical anions, e.g., $HgTe_2^{2-}$,[2] $SnTe_4^{4-}$,[3] and $As_2Se_6^{2-}$.[4] There also exist a number of solid-state structural findings on Zintl phases that contain classically bonded anions prepared by conventional means other than Corbett's alloy extraction technique (vide infra). The bulk of this work has been summarized in two recent reviews.[5]

In the most recent studies in our laboratory, the extraction of Zintl phases in ethylenediamine (en) or liquid ammonia in the presence of 2,2,2-crypt (4,7,13,16,21,24-hexaoxa-1,10-diazabicyclo[8.8.8]hexacosane) has given rise to solutions containing $HgCh_2^{2-}$, $SnCh_3^{2-}$, $TlCh_3^{3-}$, $SnCh_4^{4-}$, and $Tl_2Ch_2^{2-}$, where Ch = Se, Te.[6] The octadentate alkali-metal-ion sequestering agent 2,2,2-crypt has been used by Corbett and his co-workers to prevent reversion of the Zintl species to their respective intermetallic phases upon isolation from the solvent medium and, in a number of instances, has led to the formation of crystalline material suitable for X-ray structure analyses. In our studies, the cryptand also serves to greatly enhance the rate of solution extraction of the alkali-metal alloy and the solubility of the anion species. The latter factor is of critical practical importance to the investigation of these ordinarily dilute solutions by NMR spectroscopy. Consequently, all of the aforementioned species have been characterized in solution by direct NMR observation of the naturally abundant and/or enriched spin-$^1/_2$ isotopes $^{203,205}Tl$, ^{199}Hg, ^{119}Sn, ^{77}Se, and ^{125}Te. Multinuclear magnetic resonance spectroscopy has proven to be well-suited to the rapid and representative characterization of the chemistry of solution extracts of Zintl anions by virtue of the fact that every post-transition-metal element capable of forming a Zintl phase possesses at least one naturally abundant NMR-active isotope, which, by virtue of its nonquadrupole nature, can provide additional valuable structural information based upon its hetero- or homonuclear spin–spin couplings.

[†] McMaster University.
[‡] University of Toronto.

(1) Corbett, J. D. *Chem. Rev.* **1985**, *85*, 383.
(2) Burns, R. C.; Corbett, J. D. *Inorg. Chem.* **1981**, *20*, 4433.
(3) (a) Rudolph, R.; Wilson, W. L.; Taylor, R. C. *J. Am. Chem. Soc.* **1981**, *103*, 2480. (b) Eisenmann, B.; Schäfer, H.; Schrod, H. *Z. Naturforsch., B: Anorg. Chem., Org. Chem.* **1983**, *38B*, 921.
(4) Belin, C. H. E.; Charbonnel, M. M. *Inorg. Chem.* **1982**, *21*, 2504.
(5) (a) Krebs, B. *Angew. Chem., Int. Ed. Engl.* **1983**, *22*, 113. (b) Schäfer, H.; Eisenmann, B. *Rev. Inorg. Chem.* **1981**, *3*, 29.
(6) Burns, R. C.; Devereux, L. A.; Granger, P.; Schrobilgen, G. J. *Inorg. Chem.* **1985**, *24*, 2615.

0020-1669/87/1326-0741$01.50/0